ELSEVIER

Thermochimica Acta 335 (1999) 43–53

thermochimica acta

www.elsevier.com/locate/tca

Secondary catalytic reactions during thermal decomposition of oxalates of zinc, nickel and iron(II)

R. Majumdar*, P. Sarkar, U. Ray, M. Roy Mukhopadhyay

Department of Chemical Technology, Calcutta University, 92, A.P.C Road, Calcutta-700009, India

Received 29 September 1998; accepted 27 May 1999

Abstract

Thermal decomposition of the oxalates of zinc, nickel and iron(II) have been reexamined from a fresh experimental approach. Differential thermal analysis (DTA) and thermogravimetry (TG) of the individual oxalates and of mixtures of zinc oxalate with either nickel/iron oxalate or products of decomposition of the latter two, were carried out in air in sample cells made of different materials (Pt, Al, Al_2O_3, Ni). The information gathered from thermoanalytical experiments, together with information derived from specific chemical tests for the evolution of carbon monoxide during decomposition, chemical analyses, XRD and stoichiometric and thermochemical considerations helped to specify some of the inadequately explained features of the courses and kinetics of decomposition of the metal oxalates. Demonstrative evidence strongly indicates that secondary exothermic oxidation of carbon monoxide liberated in situ, takes place at relatively low temperatures in the presence of Pt (sample cell material), NiO and Fe_3O_4 (decomposition products) which act as catalysts and are reflected in overall exothermic DTA responses that are endothermic in air/oxygen in the absence of catalyst surfaces.

Keywords: Oxalates; Thermal decomposition; Thermal analysis; Catalyst

1. Introduction

Dollimore [1] has reviewed thermal decomposition of metal oxalates and has discussed the possible variations in the nature of DTA responses (endothermic or exothermic), the nature of products, etc. depending on the conditions of experiment. It has been generally recognised that, for many simple and complex oxalates, endothermic decomposition in nitrogen becomes exothermic in air which has been explained as arising from catalytic conversion of carbon monoxide to carbon dioxide, with the solid product providing the catalytic surface. In the case of magnesium oxalate, the catalytic effect was attributed to platinum, the material of construction of the sample cell [2].

Thermoanalytical studies on decomposition of hydrated zinc oxalate [3–6], nickel oxalate [7–11], and iron(II) oxalate [3,8,11–18] have well documented the variable nature of the products of decomposition and of DTA responses, depending on the experimental conditions. All three of the metal oxalates are also known to exhibit endothermic decarboxylation steps in oxygen-free environment that change into exothermic ones in air/oxygen. For zinc oxalate, this ‘endothermic-to-exothermic change’ has been explained as arising from secondary oxidation of carbon monoxide catalysed by zinc oxide, both being

---

*Corresponding author.

PII: S0040-6031(99)00128-8

products of decomposition [1,6]. For nickel oxalate, the effect has been attributed to highly exothermic oxidation of finely divided metallic nickel initially formed [1,9]. In iron(II) oxalate, the DTA response in air is more complicated: usually a low temperature endothermic dehydration is quickly overshadowed by a strong exothermic reaction which has been variously described as due to 'oxidation' and/or 'oxidative decomposition' [1,19].

Appropriate experimental evidences in support of the explanations offered for the referred 'endothermic-to-exothermic' DTA responses are, however, either inadequate or lacking. Any attempt to provide such supportive evidences would also entail more detailed elucidation of the thermal path of respective decomposition which is of much practical significance.

In the present study, thermal decomposition of zinc, nickel and iron(II) oxalates have been reexamined from a fresh experimental approach in order to provide supportive evidences for catalytic or other exothermic reactions responsible for the said 'endothermic-to-exothermic' responses, and concurrently, to gain more insight into the courses of thermal decomposition of metal oxalates.

2. Experimental

1. Oxalates of Zn, Ni(II), Fe(II) were prepared by precipitation from solutions of the corresponding metal sulphates with potassium oxalate (both A.R. grade). The composition and purity of the solid oxalates were established by chemical analysis and XRD. The oxalates could be represented as $MO_x{\cdot}2H_2O$ (M = Zn/Ni/Fe(II), $O_x = C_2O_4{}^{2-}$).
2. Products of decomposition of $NiO_x{\cdot}2H_2O$ and $FeO_x{\cdot}2H_2O$ obtained as residues after heating in air/nitrogen (oxygen-free)/CO_2 at ~500°C, were separately prepared for subsequent use. These products were examined by chemical analysis and XRD.
3. Differential thermal analysis and thermogravimetry were carried out with air (static) as ambient atmosphere. Two different models (DT 40 and DT 50) of the auto-recording type thermal analyser from Shimadzu (Japan) were used. Pt and Al sample cells were used with DT 40 and only alumina sample cells were used with the DT 50 equipment. In both the cases, Pt/Pt–Rh thermocouples were outside the sample. One manual DTA unit with nickel sample cell and Chromel–Alumel thermocouple (embedded in sample material) was also used. In all DTA experiments, the reference was α-alumina. Heating rates were 5/10°C min^{-1}.
4. Thermal analyses (DTA and TG) were carried out on (i) individual metal oxalates, (ii) mixtures of two metal oxalates, (iii) residual products of decomposition of Ni/Fe(II) oxalate as indicated in (2) above, and (iv) mixtures of zinc oxalate and products of decomposition of Ni/Fe(II) oxalates.
5. Ditte's tests were performed by allowing the gases evolved on heating (up to 500°C) various samples as mentioned in (4) above in a glass container under air/CO_2/N_2 flowing at slow rates, to pass through a glass bulb containing a paste of I_2O_5 and 60% oleum supported on glass wool and maintained at 80°C for possible detection of CO by liberating purple iodine ($I_2O_5 + 5CO \rightarrow I_2 + 5CO_2$) vapour.
6. For XRD, Philips PW1710 was used.

3. Results

Experimental observations are presented in Tables 1–4 and Figs. 1–10.

Relevant information regarding residual products of decomposition of nickel and iron(II) oxalates are shown in Table 1.

Table 2 and Figs. 1–5 summarise the results of thermal analyses[1] (TG and DTA) on oxalates—individual and mixtures.

Major features of thermal analyses (TG and/or DTA) of product residues (NRO, NRC, IRO, IRC, and IRN as identified in Table 1) and their mixtures with $ZnO_x{\cdot}2H_2O$ are presented in Table 3 and Figs. 6–10.

Table 4 summarises the observations made during Ditte's test for detecting evolution of carbon monoxide while heating (up to 500°C) the oxalates in flowing air/CO_2/N_2 (oxygen-free).

---

[1] Note: The thermoanalytical curves as recorded on DT 40 do not conform to the preferred plotting norms. For the sake of precision, attempts have not been made to change them.

Table 1
Residual products of thermal decomposition of $NiO_x·2H_2O$ and $FeO_x·2H_2O$

Starting oxalate, wt (mg), temperature (°C), environment	Weight of residue (mg), wt% of oxalate, colour, identity	Comments
1. $NiO_x·2H_2O$, 110.3, $\sim$500, air	43.9, 39.8, black, NRO	
2. $NiO_x·2H_2O$, 105.8,$\sim$500, CO_2	35.8, 33.8, grey, NRC	NRO and NRC were predominantly NiO and Ni, respectively (chemical analysis and XRD)
3. $FeO_x·2H_2O$, 100.5, $\sim$500, air	44.5, 44.2, brown, IRO	
4. $FeO_x·2H_2O$, 510.2, $\sim$500, CO_2	219.1, 42.9, black, IRC	the black residues IRC and IRN dissolve in dil. H_2SO_4, yielding greenish solution in which Fe^{++} could be estimated by permanganate titration; however, solution of IRC leaves some undissolved fine black particles even on boiling
5. $FeO_x·2H_2O$, 515.0, $\sim$500, N_2	226.6, 43.2, black, IRN	

Table 2
TG and DTA of oxalates—individual and mixtures

Sample	Cell material, equipment	Figure No.	Features	Comments
1. $ZnO_x·2H_2O$	(a) alumina (DT 50)	1(a)	two endothermic DTA peaks	same with Al and Ni sample cells
	(b) Pt (DT 40)	1(b)	one endo- and one exothermic DTA peaks	same when Pt is kept in contact with sample in Al cell
2. $NiO_x·2H_2O$	alumina (DT 50)	2	One endo- and one exothermic DTA peaks	same in all cells
3. $FeO_x·2H_2O$	Alumina (DT 50)	3	Combined endo-exothermic DTA peak	same in all cells
4. $ZnO_x·2H_2O + NiO_x·2H_2O$				
(a) 1 : 1 mixture	Pt (DT 40)	4(a)	exothermic DTA peak for decarboxylation of ZnO_x	same in all cells
(b) 9 : 1 mixture	Al (DT 40)	4(b)	exothermic DTA peak for decarboxylation of ZnO_x	same in all cells
5. $ZnO_x·2H_2O$ + $FeO_x·2H_2O$ (1 : 1)	Alumina (DT 50)	5	exothermic DTA peak for decarboxylation of ZnO_x	same in all cells

Table 3
TG and/or DTA of product residues of $NiO_x·2H_2O$ and $FeO_x·2H_2O$ and their mixtures with $ZnO_x·2H_2O$

Sample	Cell material, equipment	Figure No.	Features	Comments
1. NRC	alumina, DT 50	6	TG wt-gain	
2(a) IRC	alumina, DT 50	7(a)	TG wt-gain	
2(b) IRN	alumina, DT 50	7(b)	TG wt-gain	
3(a) $ZnO_x·2H_2O$ + NRO (10%)	alumina, DT 50	8(a)	exothermic DTA peak for decarboxylation of ZnO_x	
3(b) $ZnO_x·2H_2O$ + NRC (10%)	alumina, DT 50	8(b)	endothermic DTA peak for decarboxylation of ZnO_x	
4. $ZnO_x·2H_2O$ + IRO (7%)	Al, DT 40	9	endothermic DTA peak for decarboxylation of ZnO_x	
5. $ZnO_x·2H_2O$ + IRC (13%)	alumina, DT 50	10	exothermic DTA peak for decarboxylation of ZnO_x	same for mixture of $ZnO_x·2H_2O$ and IRN (7%)

Table 4
Evolution of carbon monoxide from oxalates (Ditte's test)

Sample, weight, experimental conditions	CO evolution	Colour of residue
1. $ZnO_x{\cdot}2H_2O$, 30 mg, air/CO_2/N_2	yes	yellowish white
2. $ZnO_x{\cdot}2H_2O$, 30 mg + pieces of Pt-foil, air	no	yellowish white
3. $NiO_x{\cdot}2H_2O$, 50 mg, air/CO_2	no	black in air (NRO), grey in CO_2 (NRC)
4. $ZnO_x{\cdot}2H_2O$, 50 mg + NRO, 5 mg, air	no	grey
5. $ZnO_x{\cdot}2H_2O$, 50 mg + NRC, 5 mg, air	yes	grey
6. $FeO_x{\cdot}2H_2O$, 50 mg, air	no	brown (IRO)
7. $FeO_x{\cdot}2H_2O$, 50 mg, CO_2/N_2	yes	black (IRC/IRN)

4. Discussion

4.1. Zinc oxalate

TG and DTA of zinc oxalate in air clearly indicate (Fig. 1(a and b)) that there are two corroborating steps due to dehydration and decarboxylation and the end product is always ZnO. The first DTA signal was always endothermic irrespective of the material of construction of the sample cell, but the second DTA signal was exothermic only when the sample cell was made of Pt (Fig. 1(b)), or when a few pieces of Pt-foil was mixed with zinc oxalate in the aluminium sample cell. Ditte's test always responded positively, that is CO was evolved on heating $ZnO_x{\cdot}2H_2O$ in air/CO_2/N_2 when the sample was not in contact with Pt (Table 4). All information suggests that Pt catalyses oxidation of CO liberated by ZnO_x.

Based on standard heats of formation of ZnC_2O_4 [20] and other components, thermochemical calculations indicate that the two possible decomposition

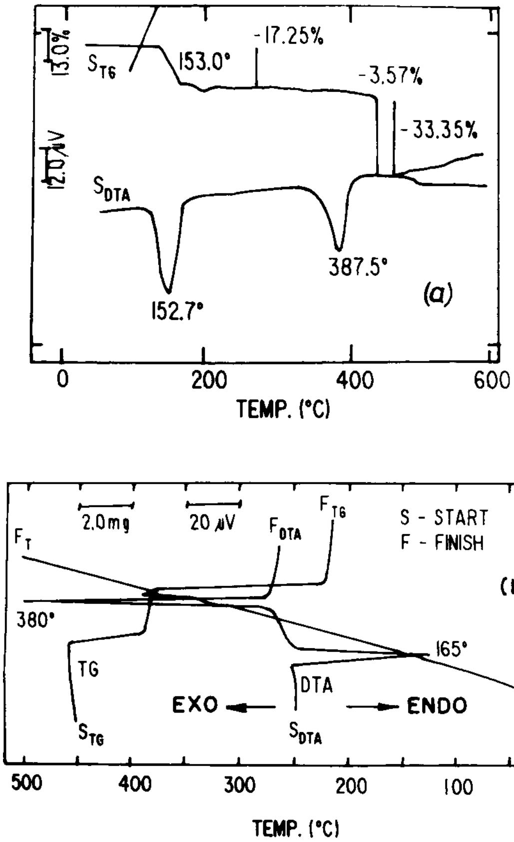

Fig. 1. TG-DTA of $ZnO_x{\cdot}2H_2O$: (a) 18.6 mg, 10°C min^{-1}, alumina cell (DT 50, Shimadzu); and (b) 20 mg, 10°C min^{-1}, Pt cell (DT 40, Shimadzu).

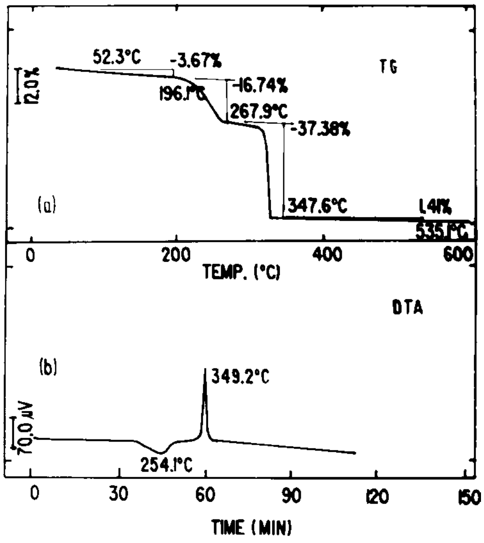

Fig. 2. TG-DTA of $NiO_x{\cdot}2H_2O$: 18.2 and 29.0 mg (for TG and DTA, respectively), 5°C min^{-1}, alumina cell (DT 50, Shimadzu).

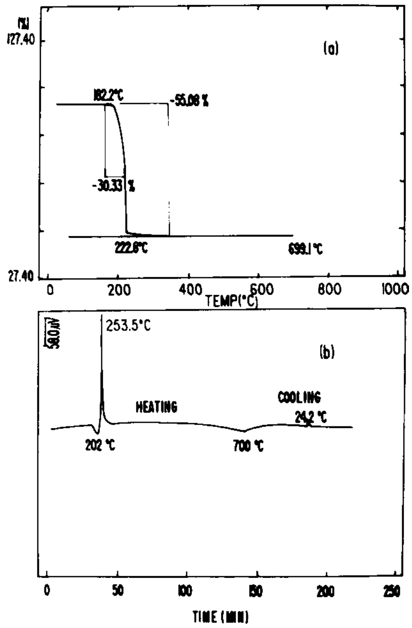

Fig. 3. TG-DTA of $FeO_x{\cdot}2H_2O$: (a) TG: 12.9 mg; (b) DTA (with cooling): 15.4 mg, 5°C min^{-1}, alumina cell (DT 50, Shimadzu).

reactions, namely

$$ZnC_2O_4 \rightarrow Zn + 2CO_2,\ \Delta H_1^0 = +201.66\,kJ \quad (1)$$

$$ZnC_2O_4 \rightarrow ZnO + CO + CO_2,\ \Delta H_2^0 = +136.73\,kJ \quad (2)$$

should be endothermic. Secondary in situ oxidation of either metallic zinc ($\Delta H = -347.98$ kJ mol^{-1}) or carbon monoxide ($\Delta H = -283.05$ kJ mol^{-1}) would result in an overall exothermic effect.

As the final product of decomposition of zinc oxalate in oxygen-free nitrogen [3] and in NH_3-N atmosphere [21] is zinc oxide, and as CO is evolved in both, oxidising and non-oxidising environment (Table 4), it is certain that the decomposition proceeds primarily via reaction (2) under all conditions. The absence of CO in evolved gases from Zn-oxalate in contact with Pt with adequate supply of air and the exothermic nature of second DTA signal under these conditions can, thus, be explained only in terms of low-temperature oxidation of CO, catalysed by Pt and not by the product ZnO.

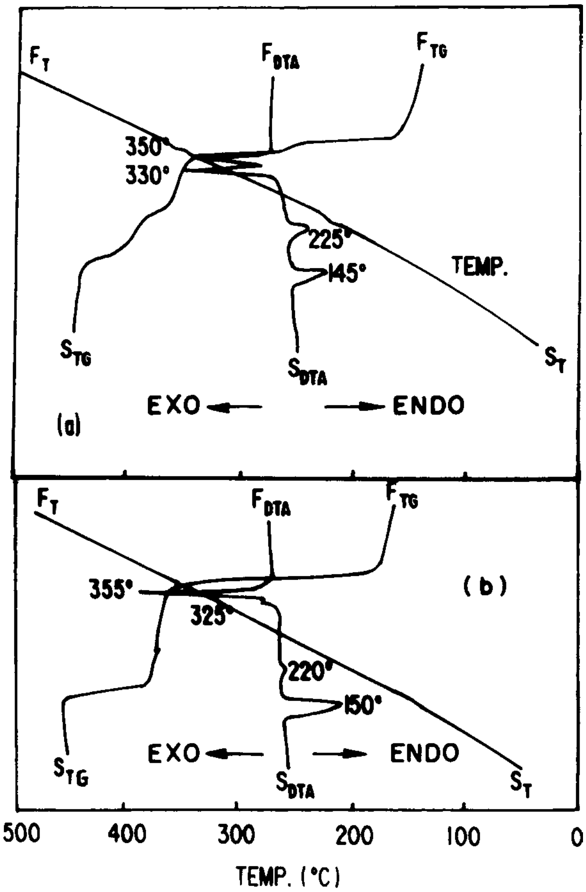

Fig. 4. TG-DTA of $ZnO_x{\cdot}2H_2O + NiO_x{\cdot}2H_2O$: (a) 1 : 1 mixture 10.0 mg, 5°C min^{-1}, Pt cell (DT 40, Shimadzu); and (b) 9 : 1 mixture 10.1 mg, 5°C min, Al cell (DT 40, Shimadzu).

4.2. Nickel oxalate

Unlike zinc oxalate, the nature of DTA responses due to thermal decomposition of nickel oxalate is not affected by sample cell materials (Table 2, Fig. 2). In air ambient atmosphere, the first step of decomposition corresponds to stoichiometric loss of water and is endothermic, and the second step corresponds to stoichiometric loss accounting for the formation of NiO as the end product and is exothermic. However, in CO_2, nickel oxalate forms a grey magnetic product (Table 3) which turns into a stable, black NiO with considerable wt-gain between ~380° and ~580°C (Fig. 6). Further, there is no indication of CO in the

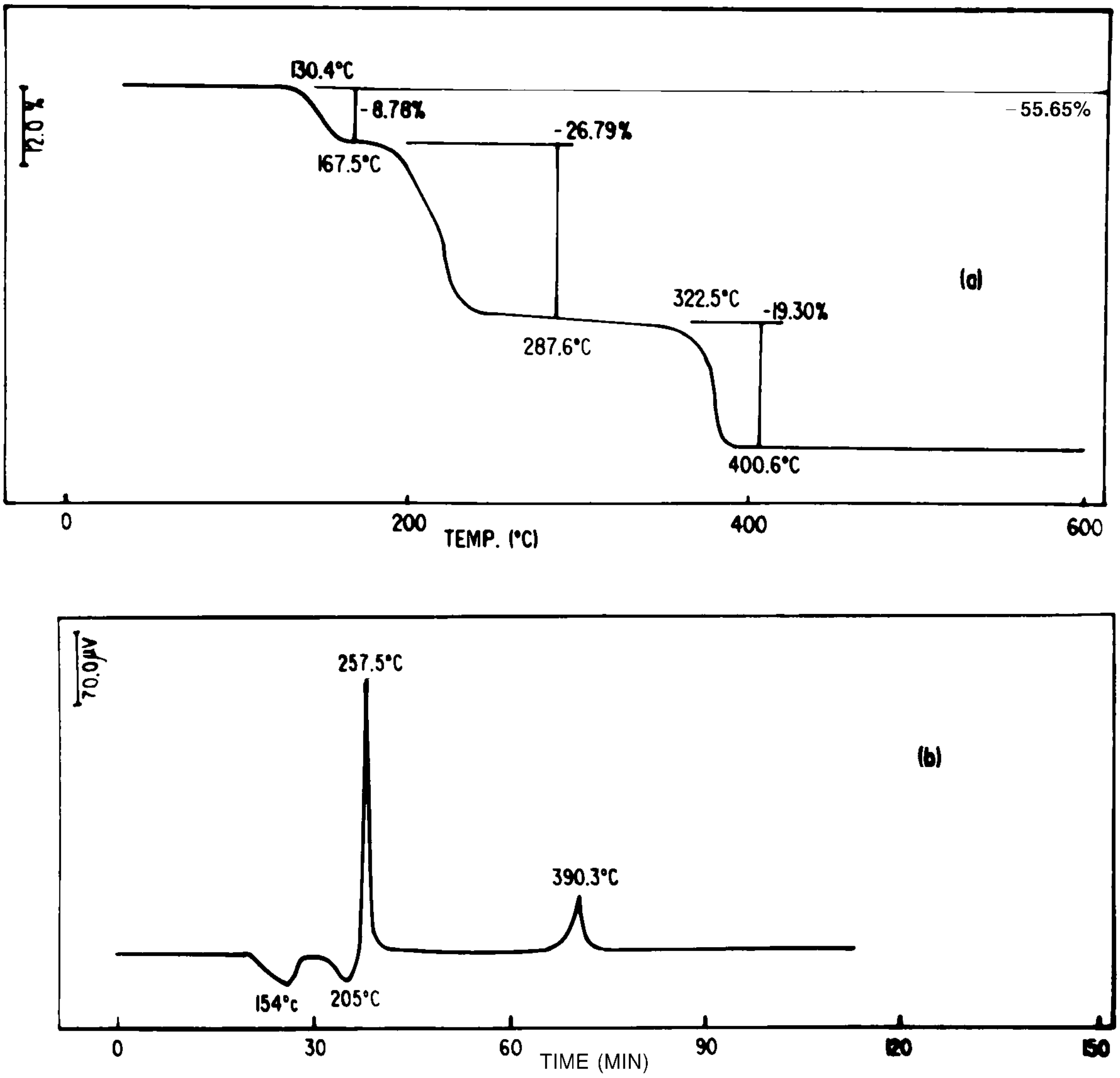

Fig. 5. TG-DTA of $ZnO_x{\cdot}2H_2O + FeO_x{\cdot}2H_2O$ (1 : 1): (a) TG: 17.4 mg; and (b) DTA: 29.0 mg, 5°C min^{-1}, alumina cell (DT 50, Shimadzu).

evolved gases from nickel oxalate heated in air or in CO_2 (Table 4).

Based on standard heats of combustion of hydrogen, carbon and oxalic acid, the standard heat at infinite dilution of oxalic acid, and the standard heat of formation Ni^{++} [20], the standard heat of formation of NiC_2O_4 could be calculated as -879.05 kJ mol^{-1} at the minimum. The possible decarboxylation reactions should, thus, have thermal effects as follows:

$$NiC_2O_4 \rightarrow Ni + 2CO_2, \quad \Delta H_3^0 = +92.05\,\text{kJ} \qquad (3)$$

$$NiC_2O_4 \rightarrow NiO + CO + CO_2, \quad \Delta H_4^0 = +133.88\,\text{kJ} \qquad (4)$$

The experimental observations, noted above, clearly suggest that the decarboxylation of nickel oxalate proceeds via reaction (3) forming metallic nickel, in an oxygen-free environment, whereas in

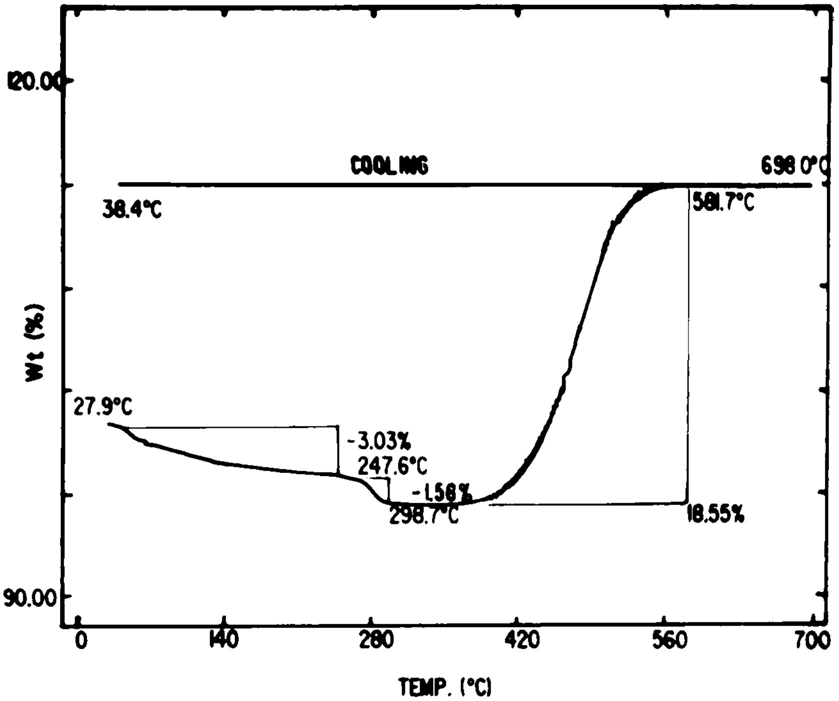

Fig. 6. TG of residue of $NiO_x{\cdot}2H_2O$ in CO_2 (NRC): 10.35 mg, 5°C min^{-1}, alumina cell (DT 50, Shimadzu).

air/oxygen, the most probable reaction appears to be an overall exothermic oxidative decarboxylation:

$$NiC_2O_4 + \tfrac{1}{2}O_2 \rightarrow NiO + 2CO_2,$$
$$\Delta H_5^0 = -149.95\,\mathrm{kJ} \qquad (5)$$

rather than the stepwise formation of metallic nickel first and its subsequent oxidation.

Of greater interest, probably, is the information revealed by the thermal analyses of mixture of $ZnO_x{\cdot}2H_2O$ and $NiO_x{\cdot}2H_2O$ (Fig. 4(a) and (b)). TG weight loss corresponds to the final composition of (NiO + ZnO) and the DTA signals clearly exhibit features characteristic of individual oxalates. It is seen (Fig. 4(b)) that oxidative decarboxylation of NiO_x takes place prior to the decarboxylation of ZnO_x and the DTA signal due to the latter reaction is exothermic even when the sample cell was not of Pt. The conclusion, therefore, follows that NiO, as a product of decomposition of NiO_x, has the same catalytic influence on low-temperature oxidation of CO liberated by ZnO_x as that of Pt.

The catalytic role of the residual product of $NiO_x{\cdot}2H_2O$ in air (NRO), is further demonstrated by the DTA of its mixture with $ZnO_x{\cdot}2H_2O$ (Fig. 8(a)). In contrast, the residual product from $NiO_x{\cdot}2H_2O$ in CO_2 (NRC) could not bring about exothermic DTA signal for decarboxylation of ZnO_x; oxidation of discrete particulate Ni takes place in small localised exothermic bursts producing ‘oscillations’ on the DTA curve and even reducing the endothermic effect due to decarboxylation of ZnO_x (Fig. 8(b)).

4.3. Iron(II) oxalate

The information of interest relating to thermal decomposition of iron(II) oxalate, may be summarised as follows:

1. Chemically estimated Fe(II) proportions in IRC, IRN and IRO (the end residues of $FeO_x{\cdot}2H_2O$ in CO_2, N_2 and air) were equivalent to 75%, 66% and 5% Fe_3O_4 respectively. TG wt-gain of IRC (2.74%, Fig. 7(a)), if attributed to $Fe_3O_4 \rightarrow Fe_2O_3$, yields 79.4% Fe_3O_4 in IRC and that of

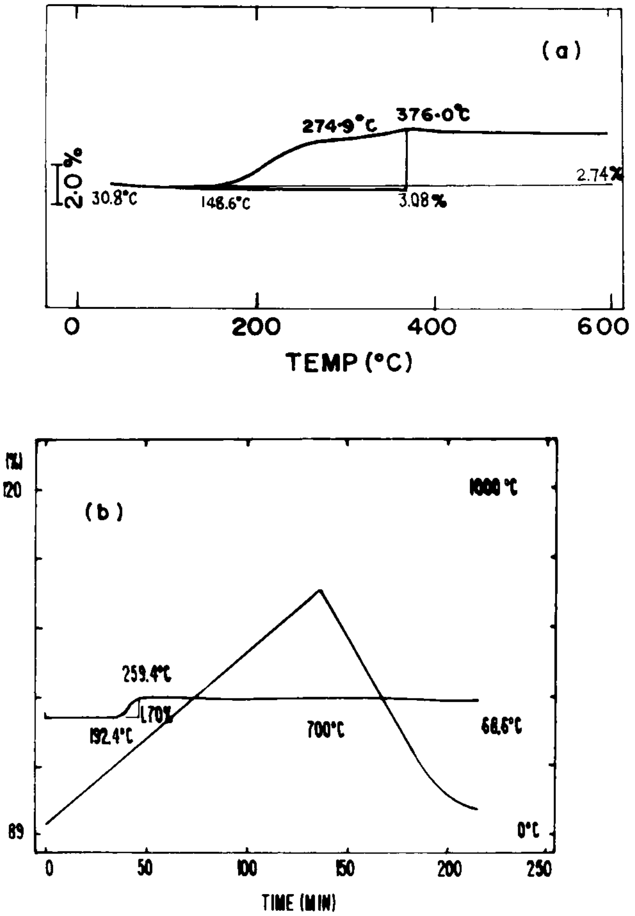

Fig. 7. (a) TG of residue of $FeO_x{\cdot}2H_2O$ in CO_2 (IRC): 10.0 mg; and (b) TG of residue of $FeO_x{\cdot}2H_2O$ in N_2 (IRN): 9.3 mg, 5°C min^{-1}, alumina cell (DT 50, Shimadzu).

IRN (1.78%, Fig. 7(b)) corresponds to 52% Fe_3O_4. XRD also indicated that while IRC, and IRN were predominantly Fe_3O_4, IRO was mainly Fe_2O_3.

2. In a 1 : 1 mixture of $ZnO_x{\cdot}2H_2O$ and $FeO_x{\cdot}2H_2O$, the thermal decomposition in air of FeO_x takes place prior to the decarboxylation of ZnO_x and the DTA signal due to the latter is rendered exothermic in non-platinum sample cells; the corresponding DTA signal for ZnO_x itself is endothermic (Fig. 5 vs. Fig. 1, Table 2).
3. The DTA responses due to decarboxylation of ZnO_x in air in the presence of IRC (and IRN) in non-platinum sample cells are exothermic (Fig. 10), but the same response is endothermic in the presence of IRO (Fig. 9).
4. Thermal decomposition of Fe(II) oxalate in sufficient air is not associated with the evolution of carbon monoxide, but those in CO_2/N_2 are associated with the evolution of CO (Table 4), and the end-residues in air consist mainly of Fe_2O_3 and those in CO_2 and N_2 are predominantly Fe_3O_4. None of these residues indicated the presence of Fe or FeO on XRD.

Considered together, the above observations strongly indicate that, the exothermic decarboxylation of zinc oxalate in the presence of iron(II) oxalate/IRC/IRN is primarily due to the catalytic effect of Fe_3O_4 in bringing about CO → CO_2 oxidation; Fe_3O_4 is likely to maintain its existence at temperatures >350°C (Fig. 7), especially when it is in admixture with larger

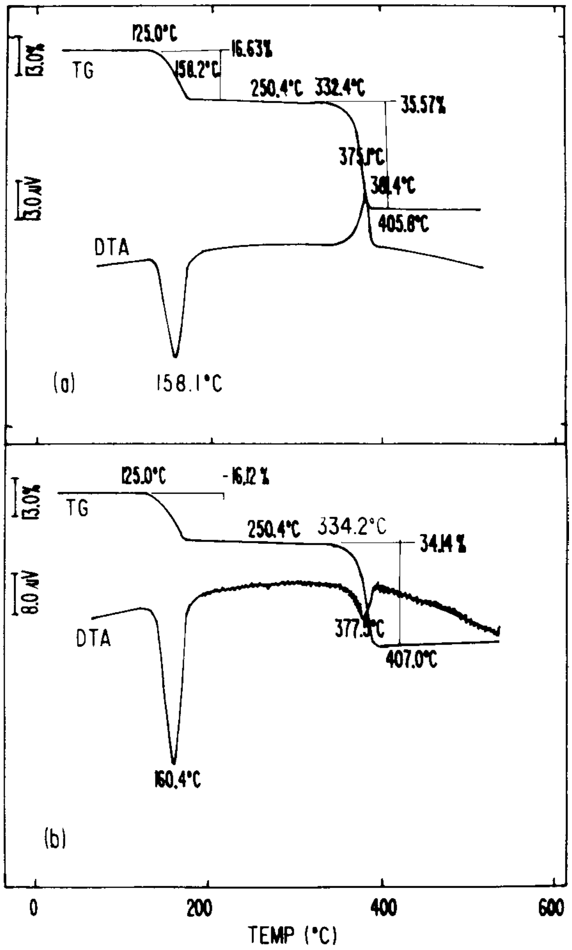

Fig. 8. TG-DTA of (a) mixture of $ZnO_x \cdot 2H_2O$ and residue of $NiO_x \cdot 2H_2O$ in air, NRO (10%), 18.4 mg; and (b) mixture of $ZnO_x \cdot 2H_2O$ and NRC(10%), 18.2 mg; 5°C min^{-1}, alumina cell (DT 50, Shimadzu).

proportions of ZnO_x, in which case it is not easily amenable to oxidation, except at the surfaces.

Based on standard heat of formation of Fe^{++} (std. st., $m = 1$, aq.) and the standard heats of combustion of oxalic acid and other components [20], the standard heat of formation of anhydrous FeC_2O_4 could be calculated as −924.34 kJ mol^{-1}, which closely agrees with the value of ΔH_f^0 (-949 ± 30 kJ mol^{-1}) calculated by Coetzee et al. [11] based on experimental DSC values of enthalpy of reaction in oxygen, assuming Fe_2O_3 and CO_2 as the end-products.

Theoretically, decomposition of ferrous oxalate in the absence of oxygen, can proceed via the following

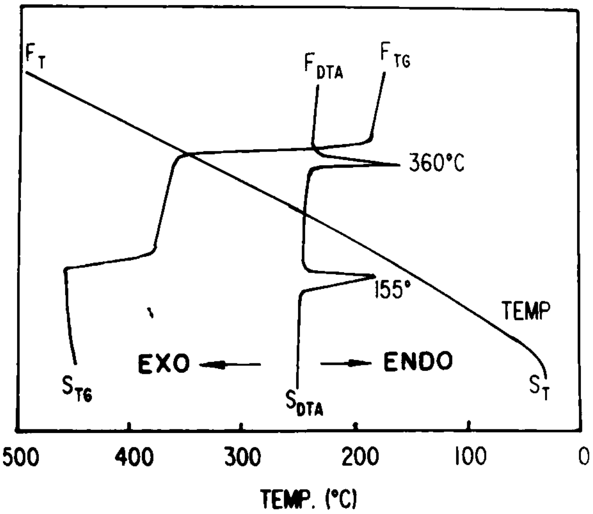

Fig. 9. TG-DTA of $ZnO_x \cdot 2H_2O$ and residue of $FeO_x \cdot 2H_2O$ in air, IRO (7%), 10.0 mg, 5°C min^{-1}, Al cell, (DT 40, Shimadzu).

possible routes:

$$FeC_2O_4 \rightarrow FeO + CO + CO_2 \quad \Delta H_6^0 = +149.8\,\text{kJ} \qquad (6)$$

$$FeC_2O_4 \rightarrow Fe + 2CO_2 \quad \Delta H_7^0 = +137.2\,\text{kJ} \qquad (7)$$

$$FeC_2O_4 \rightarrow \tfrac{1}{4}Fe + \tfrac{1}{4}Fe_3O_4 + CO + CO_2, \quad \Delta H_8^0 = +141.0\,\text{kJ} \qquad (8)$$

$$FeC_2O_4 \rightarrow \tfrac{1}{3}Fe + \tfrac{1}{3}Fe_2O_3 + CO + CO_2 \quad \Delta H_9^0 = +143.1\,\text{kJ} \qquad (9)$$

$$FeC_2O_4 \rightarrow \tfrac{1}{2}Fe_2O_3 + \tfrac{3}{2}CO + \tfrac{1}{2}CO_2, \quad \Delta H_{10}^0 = +146.4\,\text{kJ} \qquad (10)$$

$$FeC_2O_4 \rightarrow \tfrac{1}{3}Fe_3O_4 + \tfrac{4}{3}CO + \tfrac{2}{3}CO_2, \quad \Delta H_{11}^0 = +139.5\,\text{kJ} \qquad (11)$$

(values of ΔH^0 for the reactions were estimated on the basis of calculated ΔH_f^0 of FeC_2O_4 (−924.34 kJ mol^{-1}) and ΔH_f^0 of other products).

Values of ΔH^0 for all the possible reactions are endothermic and are of the same order of magnitude. But, in view of the fact that no Fe could be detected in IRC and IRN, reactions (7), (8) and (9) seem improbable. Moreover, CO is evolved from FeO_x when heated in CO_2 and N_2 (Table 4), supporting the improbability

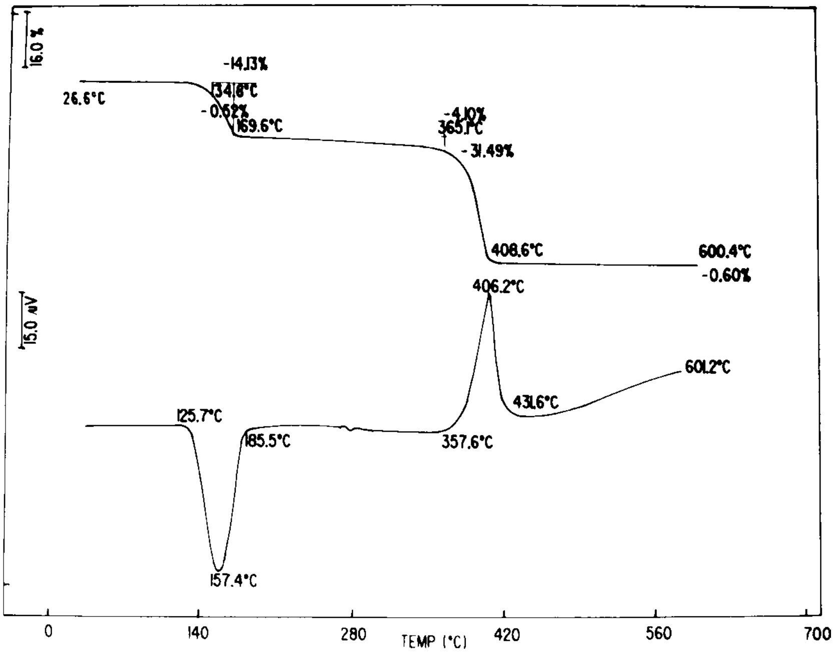

Fig. 10. TG-DTA of mixture of $ZnO_x{\cdot}2H_2O$ + IRC (13%), 11.5 mg and 11.7 mg for TG and DTA, respectively: 5°C min^{-1}, alumina cell (DT 50, Shimadzu).

of reaction (7) under those conditions. Reaction (6) is unlikely, because neither the black residues in CO_2 and N_2 nor the brown residue in air indicated the presence of FeO by XRD. Even if FeO would disproportionate [19,22], $4FeO \rightarrow Fe + Fe_3O_4$, ΔH: +35.15 kJ or, $3FeO \rightarrow Fe + Fe_2O_3$, ΔH: +19.25 kJ, there would be Fe present in the residues. We are, therefore, inclined to consider that the decomposition reactions proceed via routes (10) and/or (11). Coetzee et al [11] also could not detect Fe in the decomposition products of FeO_x, but could detect Fe_3O_4 by thermomagnetometry. Rane et al. [18] detected Fe_3O_4 in the decomposition products by dynamic measurement of electrical resistivity. It, thus, appears perfectly possible that, in the presence of oxygen, anhydrous FeO_x, as soon as it starts forming by dehydration, undergoes oxidative decomposition, as was suggested by Macklen [19]

$$FeC_2O_4 + \tfrac{3}{4}O_2 \rightarrow \tfrac{1}{2}Fe_2O_3 + 2CO_2,$$
$$\Delta H^0_{12} = -278.15\,\text{kJ} \qquad (12)$$

which releases the required energy to locally raise the temperature for the favourably located particles of FeO_x to be decomposed by reaction routes (10) and (11), yielding CO and CO_2. Carbon monoxide in the evolved gases, in turn, undergoes oxidation catalysed by Fe_3O_4 formed in situ

$$CO + \tfrac{1}{2}O_2 \rightarrow CO_2, \quad \Delta H^0_{13} = -283.05\,\text{kJ} \qquad (13)$$

Fe_3O_4 itself, too, is oxidised

$$2Fe_3O_4 + \tfrac{1}{2}O_2 \rightarrow 3Fe_2O_3,$$
$$\Delta H^0_{14} = -258.15\,\text{kJ} \qquad (14)$$

Thus, during thermal decomposition of FeO_x in air/oxygen, the overall strong exothermic DTA signal is produced by the sequential chain reactions (12)→(10) and (11)→(13) and (14).

Quantitative measurements of relative proportions of CO : CO_2 in the evolved gases made by Coetzee et al. [11] further substantiate the explanation put forth above. In N_2, the overall CO : CO_2 percent ratio was measured as 70 : 30, and the same in CO_2 (and also in vacuum) was of the order of 30 : 70. It may be noted that reactions (10) and (11) would yield CO and CO_2 in percent ratios of 75 : 25 and 66.7 : 33.3, respectively, along with Fe_2O_3 or Fe_3O_4 as solid products. The ratios of $CO : CO_2$ measured [11] and the preseuce of both Fe_3O_4 and Fe_2O_3 in IRC and IRN (present study), thus indicating that the decomposition of FeO_x is shared by reactions (10) and (11); may be, the extent of sharing is different in different environments. Other specific reactions, for example, $2CO \rightarrow CO_2 + C$, may be responsible [23] for the much lower $CO : CO_2$ overall percent ratio in environments like CO_2 as observed by Coetzee et al. [11], and for deposition of fine carbon particles on the product residues (like IRC). But these points need further exploration.

In the absence of oxygen, iron(II) oxalate dehydrates endothermically, and the initiation of chain of events indicated above is inhibited as reaction (12) does not occur and eventually FeC_2O_4 undergoes endothermic decomposition at a higher temperature [16] following reactions (10) and (11). In fact, we could induce a sharp exothermic effect by allowing air into the reaction site at any chosen temperature $>200°C$ and up to ca. 380°C, after the endothermic dehydration step was over.

5. Conclusion

The present study demonstrates that Pt as sample cell material and certain products of decomposition of metal oxalates (NiO, Fe_3O_4) can act as catalysts for secondary oxidation of evolved gases like CO and can render otherwise endothermic DTA responses overall exothermic.

These findings are expected to be helpful in interpreting the thermoanalytical observations with oxysalts in general, and oxalates in particular.

In view of the immense practical importance of oxalates and other oxysalts and of processes involving Fe–Fe oxides–CO–CO_2–H_2O, it is necessary that due consideration should be given for possible effects of co-product catalysts to obtain more detailed information about the thermal course while studying/processing materials involving relevant systems.

References

[1] D. Dollimore, Thermochim. Acta 117 (1987) 331.
[2] D. Dollimore, J. Mason, Thermochim. Acta 43 (1981) 183.
[3] D. Dollimore, D.L. Griffiths, J. Therm. Anal. 2 (1970) 229.
[4] B.D. Dalvi, A.M. Chavan, J. Therm. Anal. 14 (1978) 331.
[5] Z. Gabelica, R. Hubin, E.G. Derouane, Thermochim. Acta 24 (1978) 315.
[6] D. Dollimore, J. Therm. Anal. 11 (1977) 187.
[7] D. Broadbent, D. Dollimore, J. Dollimore, J. Chem. Soc. A (1966) 278.
[8] E.D. Macklen, J. Inorg. Nucl. Chem. 30 (1968) 2689.
[9] D. Dollimore, in: R.C. Mackenzie (Ed.), Differential Thermal Analysis, vol. 1, Academic Press, 1970, pp. 408.
[10] N. Deb, P.K. Gogoi, N.N. Das, J. Therm. Anal. 36 (1990) 465.
[11] A. Coetzee, D.J. Eve, M.E. Brown, J. Therm. Anal. 39 (1993) 947.
[12] Y.A. Ugai, Zh. Obsh. Chim. 24 (1954), 1315; Chem. Abstr. 49 (1955) 4383i.
[13] R.A. Brown, S.C. Beevan, J. Inorg. Nucl. Chem. 28 (1966) 387.
[14] D. Dollimore, D. Nicholson, J. Chem. Soc. (1962) 960.
[15] D. Dollimore, D.L. Griffith, D. Nicholson, J. Chem. Soc. (1963) 2617.
[16] D. Broadbent, D. Dollimore, J. Dollimore, J. Chem. Soc. A (1967) 451.
[17] B. Viswanathan, J. Gopalakrishnan, V. Srinivasan, J. Therm. Anal. 3 (1971) 429.
[18] K.S. Rane, A.K. Nikumbh, A.J. Mukhedkar, J. Mater. Sci. 16 (1981) 2387.
[19] E.D. Macklen, J. Inorg. Nucl. Chem. 29 (1967) 1229.
[20] CRC Handbook Chem. Phys., 70th edn. (1989–1990).
[21] Fang Youling, Zhao Wenkuan, Chen Xingfan, Tuliao Gougye 4 (1991) 4; Chem. Abstr. 116 (1992) 196275z.
[22] G.C. Nicholson, J. Inorg. Nucl. Chem. 38 (1976) 1599.
[23] Kimizuka Noboru, Takayama Eiji, Rev. Sci. Instrum. 52 (1981) 625.